

RESEARCH ARTICLE

midline represses Dpp signaling and target gene expression in *Drosophila* ventral leg development

Lindsay A. Phillips, Markle L. Atienza, Jae-Ryeon Ryu, Pia C. Svendsen, Lynn K. Kelemen and William J. Brook*

ABSTRACT

Ventral leg patterning in *Drosophila* is controlled by the expression of the redundant T-box Transcription factors *midline* (*mid*) and *H15*. Here, we show that *mid* represses the Dpp-activated gene *Daughters against decapentaplegic* (*Dad*) through a consensus T-box binding element (TBE) site in the minimal enhancer, *Dad13*. Mutating the *Dad13* DNA sequence results in an increased and broadening of *Dad* expression. We also demonstrate that the engrailed-homology-1 domain of *Mid* is critical for regulating the levels of phospho-Mad, a transducer of Dpp-signaling. However, we find that *mid* does not affect all Dpp-target genes as we demonstrate that *brinker* (*brk*) expression is unresponsive to *mid*. This study further illuminates the interplay between mechanisms involved in determination of cellular fate and the varied roles of *mid*.

KEY WORDS: Tissue patterning, Limb development, Dpp-signaling, T-box transcription factors

INTRODUCTION

Proper organization of tissue is crucial for maintaining the body plan of animals. This organization occurs during development when multiple factors cooperate to determine cell fate. In particular, the *Drosophila melanogaster* leg is organized in part by the interplay between signaling molecules and transcription factors. Dorsal and ventral fates in *Drosophila* legs are dependent on the action of morphogens and selector genes. The morphogens decapentaplegic [*dpp*, a bone morphogenetic protein (BMP) homolog] and *wingless* (*wg*, a fly Wnt) are induced by Hedgehog signaling. *Wg* is induced in the ventral domain and controls ventral fate through induction of the redundant Tbx20 class T-box transcription factor homologs *midline* (*mid*) and *H15*, that specify ventral fate (Svendsen et al., 2009). Dorsal fate is dictated by *dpp*, which is expressed at high levels in the dorsal domain and low levels in the ventral domain, though it has no role in ventral fate aside from joint formation (Held and Heup, 1996; Manjón et al., 2007). Dpp-signaling is mediated by transcription factors Mothers against dpp (Mad), a fly Smad1/5 activator and Medea (Med), a fly Co-Smad (Hudson et al., 1998; Kim et al., 1997).

mid and *H15* control ventral patterning being both necessary and sufficient to specify the fate in the ventral region of fly legs

(Svendsen et al., 2009). They act as selector genes, transcription factors that specify cell fate for a particular developmental region, with expression restricted to the region in which they specify cell fate (Mann and Morata, 2000). The ventral specific expression of *mid* and *H15* is controlled through a combination of *Wg* activation and Dpp repression (Svendsen et al., 2009, 2015). When *mid* and *H15* function is lost in the ventral leg, tissues are transformed into dorsal while ectopic expression of *mid* or *H15* induces ventral fate in dorsal regions (Svendsen et al., 2009).

How does *mid* control ventral development? We have shown that one role of *mid* is to block Dpp signaling in the ventral domain (Svendsen et al., 2019). The distribution of phosphorylated Mad (pMad) follows the same pattern as *dpp*, with significant levels of staining in the dorsal domain and weaker staining in ventral region, indicating that the Dpp pathway is activated at lower levels in ventral cells. While Dpp does not contribute to ventral patterning, double-mutant analysis shows that the ventral to dorsal transformation of *mid H15* mutant clones in some regions of the leg is rescued to ventral phenotype if they are simultaneously blocked for Dpp signaling. This indicates an inhibitory effect of *mid* and *H15* on Dpp signaling that is necessary for ventral patterning. This is further demonstrated by the inhibition of pMad accumulation by *mid* (Svendsen et al., 2019). Additionally, *mid*-expressing clones repress the Dpp-target genes *Dad*, *Upd3*, and *mid* itself in an eh1-dependent manner, and using chromatin-immunoprecipitation (ChIP) assays, *Mid* has been shown to localize to enhancers for these genes (Svendsen et al., 2019).

Here, we study further the way *mid* antagonizes Dpp signaling, showing that it represses the regulation of *Dad*, a target gene activated by Dpp/pMad, but has no effect on *brk*, a gene repressed by Dpp/pMad. We show that *Mid* repression of *Dad* depends on a predicted T-box binding element (TBE) in the *Dad13* enhancer, and that *Mid*-inhibition of Dpp-dependent pMad accumulation and tissue re-patterning depends on the eh1 repressor domain.

RESULTS***mid* blocks Dpp activation of *Dad13* reporter expression**

Our previous work showed that the eh1 repressor binding domain was required for *Mid* selector gene function. We also showed that *Mid* acted by antagonizing Dpp signaling, reducing the levels of pMad accumulation in the ventral domain of the fly leg (Svendsen et al., 2019). Here, we further investigate how *mid* affects Dpp-target gene expression. The Dpp-target genes *Dad* and *brk* are canonical examples of genes activated or repressed by Dpp signaling, respectively (Gao et al., 2005; Tsuneizumi et al., 1997). Since *mid* antagonizes Dpp signaling, we sought to understand how *mid* regulates both genes. We showed previously that an enhancer-trap reporter of *Dad* (*Dad-lacZ*) was weakly repressed by *Mid* in an eh1-dependent manner (Svendsen et al., 2019). *Mid* likely antagonizes Dpp-target genes through direct repression because *Mid* has been shown to bind to several enhancer fragments of *Dad* in

Alberta Children's Hospital Research Institute, Department of Biochemistry and Molecular Biology, Cumming School of Medicine, University of Calgary, 3330 Hospital Drive NW, Calgary, AB T2N 4N1, Canada.

*Author for correspondence (brook@ucalgary.ca)

 W.J.B., 0000-0003-3412-4266

This is an Open Access article distributed under the terms of the Creative Commons Attribution License (<https://creativecommons.org/licenses/by/4.0>), which permits unrestricted use, distribution and reproduction in any medium provided that the original work is properly attributed.

Received 22 December 2021; Accepted 25 April 2022

ChIP assays (Svendsen et al., 2019). One of these fragments was a well-characterized 520 bp enhancer, *Dad13*. The *Dad13*-driven expression pattern is similar to that of *Dad-lacZ*, with strong expression in the dorsal domain and weaker expression in the ventral domain. However, the ventral *Dad13*-driven expression is weaker compared to wild-type *Dad*. We first confirmed that a *Dad13* reporter was regulated by *Mid*. We investigated whether loss of *H15* and *mid* function would affect *Dad13*-driven expression by generating *H15 mid* loss-of-function clones via mitotic recombination in imaginal discs of second instar larvae. *Dad13*-driven expression was detected by RFP expression while clones null for *H15 mid* were marked by the absence of GFP. Ventrally located *H15 mid* loss-of-function clones showed either an increase of *Dad13*-driven expression or an expansion into the lateral region of the leg imaginal disc (Fig. 1A,B). Because the *mid* expression domain completely encompasses the ventral *Dad13* domain (Fig. S1C), we induced ectopic Dpp-signaling in lateral regions of the imaginal disc in order to induce *Dad13*-reporter expression outside the *mid*-expression domain. We then introduced *mid* expression to assess the ability of *Mid* to repress *Dad13*. By using *AyGal4*, a construct that generates random clones expressing *Gal4* under the control of the *actin5C* promoter, we induced clones marked by GFP expression that also expressed a constitutively active form of the Dpp receptor, *thickveins* (*UAS-tkv^{QD}*) and/or expressed *Mid*. As expected, *UAS-tkv^{QD}* expressing clones, which are constitutively activated for Dpp-signaling, had increased *Dad13*-nRFP reporter expression. However, co-expressing *UAS-mid⁺* and *UAS-tkv^{QD}* blocked the ectopic activation of *Dad13*-nRFP in clones located throughout the disc (Fig. 1C,D). This indicates that the presence of *Mid* blocks the effects of Dpp-signaling on *Dad13*-driven expression. Together these results confirm that *Mid* does indeed regulate the Dpp-target gene *Dad* via its enhancer fragment, *Dad13*.

The TBE in *Dad13* is necessary for *mid* repression of *Dad*

To further investigate the role of *mid* in *Dad* regulation, we examined how *Mid* influences *Dad13*-reporter expression. The *Dad13* enhancer contains multiple binding sequences for *Mad* that are responsible for driving *Dad13* expression (Weiss et al., 2010). *Dad13* also contains tandem Smad binding element (SBE) sequences (GTCTGTCT) that have a minor role in activating *Dad13*-reporters in embryos but which have not been tested in leg imaginal discs (Weiss et al., 2010). Adjacent to the SBE sites and separated by a single nucleotide is a consensus T-box binding element (TBE) (AGGTGA) similar to the consensus binding site for *Mid* (Najand et al., 2012). To test whether the TBE is necessary for *Mid* regulation of *Dad13*, we mutated the *Dad13*-TBE site (*Dad13^{TBE}*) and tested expression with a *lacZ* reporter (Fig. 2A). *Dad13^{TBE}*-*lacZ* reporter expression was stronger and broader in the ventral domain compared to the *Dad13*-*lacZ* control (Fig. 2B,D). This clearly indicates that the TBE is required for repression of *Dad*. Furthermore, the *Dad13^{TBE}*-driven expression in dorsal regions outside the *mid* expression domain was more intense than *Dad13*-driven expression, suggesting that factors expressed outside the ventral domain may also regulate *Dad* through the TBE site. The proximity of the activating SBE next to the potential *Mid*-binding element suggested a model in which the activation of *Dad13* by Dpp may be blocked by *Mid* or other factors interfering with the SBE site. However, mutating the SBE (*Dad13^{SBE}*) had no observable effect on *Dad13*-driven expression and mutating both the TBE and SBE (*Dad13^{SBE+TBE}*) produced effects on reporter expression that were similar to mutating the TBE alone (Fig. S3). Thus, the SBE site does not appreciably affect *Dad13*-driven expression in the leg imaginal disc and the TBE site must affect *Dad13* enhancer through another mechanism.

To test whether *Mid* could still regulate *Dad13^{TBE}*-driven expression, we generated *UAS-mid⁺* gain-of-function clones and measured *Dad13^{TBE}*-*lacZ* expression. Consistent with our previous

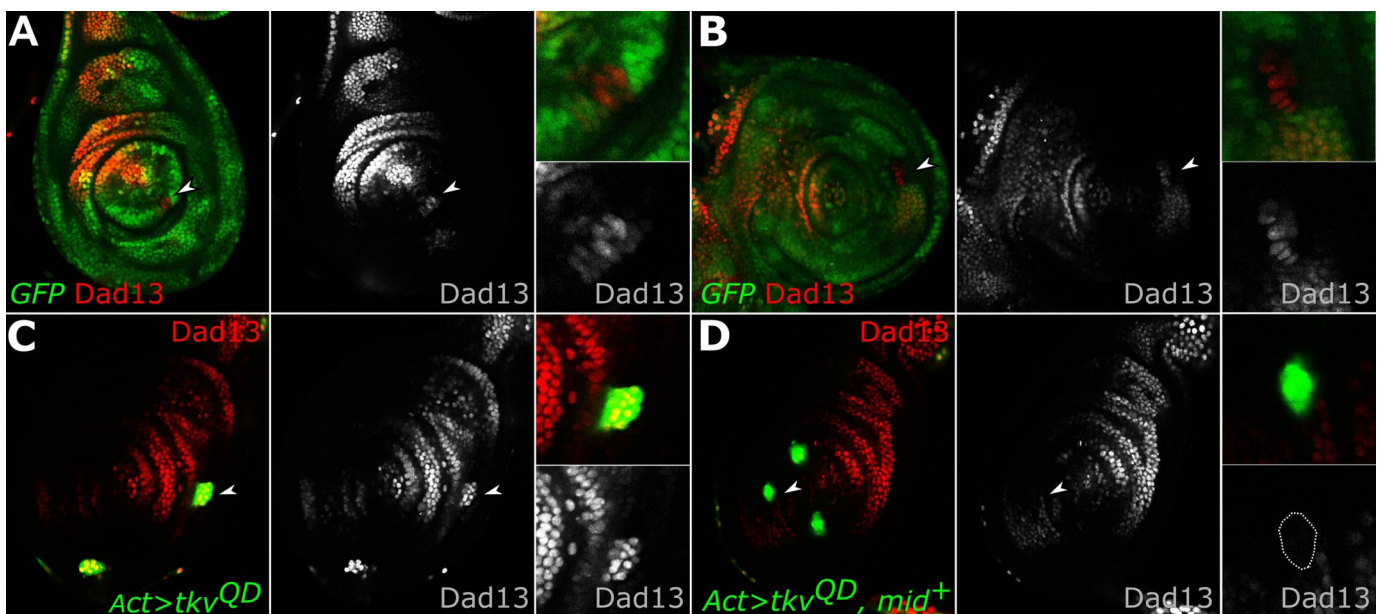


Fig. 1. *Mid* blocks Dpp activation of *Dad13*-driven expression. (A–B) Third-instar leg discs expressing *Dad13*-nRFP (red, single channel) and loss-of-function *H15* and *mid* (lack of green) clones. Clones lacking *H15* and *mid* have (A) increased *Dad13*-nRFP reporter expression (white arrowhead, lower inset), or (B) expanded *Dad13*-nRFP reporter expression (white arrowhead, lower inset; $n=7$). (C) Discs with *UAS-tkv^{QD}* gain-of-function clones (green) driven by *AyGal4* driver showed ectopic *Dad13*-driven expression (red, single channel, lower inset; $n=12$), while (D) clones co-expressing *UAS-tkv^{QD}* and *UAS-mid⁺* (green) did not induce ectopic *Dad13*-driven expression (red, single channel, lower inset clone outline; $n=13$). All imaginal discs in this report are orientated dorsal up, anterior left.

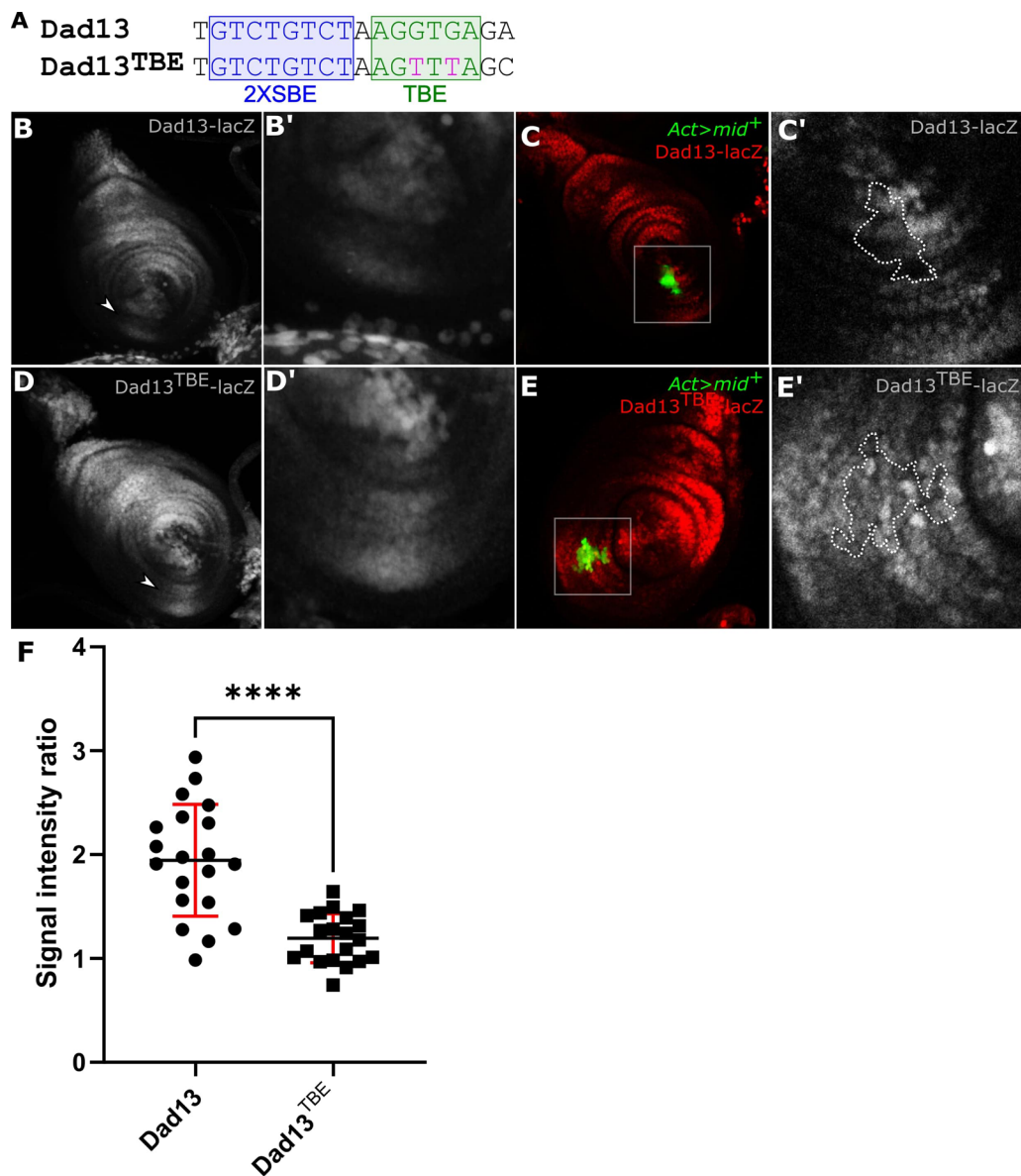


Fig. 2. Mid repressed Dad in part though the TBE. (A) Dad13 enhancer fragment sequences, showing the 2x SBE sequence (blue) and the TBE sequence (green). Two G to T substitutions in the TBE were generated for the Dad13^{TBE} construct (fuchsia). (B) Dad13 expression was detected by lacZ with strong staining in the dorsal domain and weak staining in the ventral domain (arrowhead; $n=37$). (B') Magnified image of ventral Dad13-lacZ reporter expression. (C,C') UAS-*mid*⁺ gain-of-function clones (GFP) partially repressed Dad13 expression (red channel, clone outline, C'; $n=8$). (D) Dad13^{TBE}-lacZ reporter expression is broader and more intense in the ventral domain relative to Dad13 (arrowhead). Dorsal expression driven by Dad13^{TBE} is also stronger compared to Dad13 ($n=35$). (D') Magnified image of ventral of Dad13^{TBE}-lacZ reporter expression. (E,E') Example of a UAS-*mid*⁺ gain-of-function clone (GFP) which maintains normal levels of ventral Dad13^{TBE}-lacZ reporter expression. No repression of Dad13^{TBE}-lacZ reporter expression was seen compared to adjacent regions outside the clone (red channel, outline, E'; $n=11$). (F) Fluorescent signal intensities of Dad13-lacZ and Dad13^{TBE}-lacZ for pairs of adjacent cells inside and outside of a UAS-*mid*⁺ gain-of-function clone were measured and compared to create ratios of outside/inside. Five clones were measured for each Dad13 strain (Dad13-lacZ or Dad13^{TBE}-lacZ) with two to five cell pairs being measured per *mid* clone. The overall mean ratio of cell pairs outside versus inside of a UAS-*mid*⁺ gain-of-function clone in a Dad13-lacZ leg imaginal discs was 1.95. The overall mean ratio of cell pairs outside versus inside of a UAS-*mid*⁺ gain-of-function clone in a Dad13^{TBE}-lacZ leg imaginal discs was 1.19. Statistical analysis used the Unpaired *t*-test with two-tailed *P*-value. Bars representing the mean, s.d., and significance indicated, **** P -value ≤ 0.0001 .

work (Svendsen et al., 2019), Dad13-reporter expression was repressed in most *mid*-expressing clones in the ventral domain (7/8) (Fig. 2C,C'). In contrast, few *mid*-expressing clones in the ventral domain of discs a decreased Dad13^{TBE}- driven expression (1/11 clones; Fig. 2E,E'). To further validate that *mid*-expressing clones had weaker effects on Dad13^{TBE}-reporter expression, we measured the expression in pairs of adjacent cells located inside and outside of the *mid*-expressing clone. The ratio of reporter expression of the

outside cell divided by the reporter expression of the inside cell was 1.95 for Dad13 and 1.19 for Dad13^{TBE} (Fig. 2F). These results suggest that the wild-type TBE in the Dad13 enhancer fragment is an essential element for the *mid*-mediated repression of *Dad*.

mid* does not substantially affect Dpp repression of *brk

brk is negatively regulated by Dpp signaling. Unlike *Dad*, which is activated by a complex of pMad and Med, *brk* is repressed by a

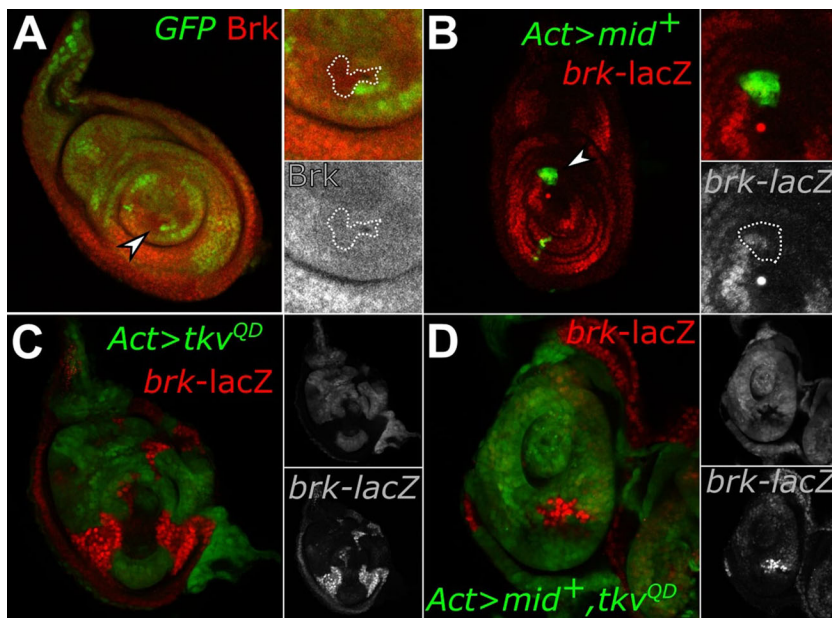


Fig. 3. Mid does not affect *brk* expression. (A) *H15 mid* loss-of-function (lack of green, arrowhead) clones have no effect on *Brk* expression, as detected by a *Brk* antibody (red, lower inset clone outline; $n=41$). (B) Discs expressing *AyGal4 UAS-mid⁺* gain-of-function clones (green) do not affect *brk-lacZ* expression, as detected by anti- β -Galactosidase staining (red, lower inset clone outline; $n=34$). (C) Clones expressing *UAS-tkv^{QD}* (green, top inset) have a dramatic repressive effect on *brk-lacZ* levels, with only residual *brk-lacZ* expression remaining (red, lower inset; $n=7$). (D) Clones co-expressing *UAS-tkv^{QD}* and *UAS-mid⁺* (green, top inset) also greatly reduce *brk-lacZ* expression, with only slightly higher remaining *brk-lacZ* expression (red, lower inset; $n=7$).

complex of pMad and Med binding along with a third protein, Schnurri, through a repressive binding element (Hamaratoglu et al., 2014; Marty et al., 2000; Saller and Bienz, 2001; Weiss et al., 2010). In leg imaginal discs, high levels of *brk* and pMad expression are reciprocal, demonstrating their antagonistic activities (Müller et al., 2003; Fig. S1). We found that neither *H15 mid* loss-of-function clones nor *mid⁺*-expressing gain-of-function clones had any effect on *brk* expression. In loss-of-function experiments, endogenous *brk* expression was detected by a *brk* antibody and remained unchanged in ventrally located clones lacking *H15 mid* (Fig. 3A, insets). Moreover, *mid⁺* gain-of-function clones marked by GFP (*UAS-mid⁺*) and located throughout the imaginal disc did not affect *brk-lacZ* expression (Fig. 3B, insets). Because Dpp-signaling represses *brk* and *mid* represses Dpp-signaling, we tested if ectopic expression of Dpp signaling with *mid* would increase or otherwise affect *brk* expression. As expected, gain-of-function clones expressing *UAS-tkv^{QD}* gain-of-function strongly repressed *brk-lacZ* reporter expression leaving only residual expression (Fig. 3C, insets). However, clones co-expressing *UAS-mid⁺* with *UAS-tkv^{QD}* had little influence on the *tkv^{QD}* gain-of-function effect on *brk*-reporter expression, which remained almost as strongly repressed (Fig. 3D, insets). This was surprising given that clones co-expressing *UAS-mid⁺* and *UAS-tkv^{QD}* have markedly reduced pMad staining compared to clones expressing *UAS-tkv^{QD}* alone (Fig. S2; Svendsen et al., 2019). This suggests that clones co-expressing *UAS-mid⁺* and *UAS-tkv^{QD}* have sufficient residual pMad activation to repress *brk* despite *UAS-mid⁺* expression. Taken together, these results suggest that *mid* does not regulate *brk* and thus *mid* does not affect all Dpp-target genes.

Mid antagonizes Dpp signaling in an eh1-dependent manner

Mid acts as a repressor through its engrailed-homology-1 (eh1) domain, which recruits the co-repressor *groucho* (*gro*) (Formaz-Preston et al., 2012). The eh1 domain is essential for Mid-mediated repression of genes in the ventral leg including the Dpp-target gene *Dad* (Svendsen et al., 2019). Here we asked if the eh1 is also necessary to inhibit the effects of ectopic Dpp signaling, including phenotypic defects and pMad accumulation. We generated gain-of-function *UAS-tkv^{QD}* clones in developing imaginal discs in second

instar larvae. In adult legs, these clones gave rise to rounded outgrowths characteristic of ectopic Dpp-signaling (Fig. 4A; Svendsen et al., 2019). Next, we co-expressed *UAS-tkv^{QD}* and a Flag-tagged *mid* (*UAS-mid⁺*-Flag) in adult legs. These clones induced fewer defects, which were less severe with generally smaller outgrowths (Fig. 4C). However, when we co-expressed *UAS-tkv^{QD}* with *UAS-mid^{eh1}*-Flag, a transgene in which the eh1 domain is mutated and has reduced Gro-binding (Formaz-Preston et al., 2012), the adult legs (Fig. 4E) displayed outgrowths similar in size and severity to clones expressing *UAS-tkv^{QD}* alone (Fig. 4A). Overall, more defects were detected in legs containing either *UAS-tkv^{QD}* or *UAS-tkv^{QD}* and *UAS-mid^{eh1}*-Flag clones as compared to legs expressing *UAS-tkv^{QD}* and *UAS-mid⁺*-Flag clones.

In addition to the different patterning defects induced in adult legs, we also saw changes in the pMad accumulation in leg imaginal discs. Clones in third-instar discs expressing gain-of-function *UAS-tkv^{QD}* have increased pMad staining (Fig. 4B,B',B''). Similar levels of pMad were detected in clones co-expressing *UAS-tkv^{QD}* and *UAS-mid^{eh1}*-Flag (Fig. 4F,F',F''). In comparison, clones expressing the *UAS-mid⁺*-Flag and *UAS-tkv^{QD}* had lower levels of pMad staining relative to the other two genotypes (Fig. 4D,D',D'', G). We note that the suppression of pMad by Flag-tagged *UAS-mid⁺*-Flag is less pronounced than the suppression by untagged *UAS-mid⁺* (Fig. S2; Svendsen et al., 2019). This is consistent with our observation that all Flag-tagged Mid gain-of-function phenotypes are weaker compared to untagged Mid (Formaz-Preston et al., 2012; Svendsen et al., 2019). However, the *UAS-mid⁺*-Flag is able to rescue *mid* mutants, and the *UAS-mid⁺*-Flag and *UAS-mid^{eh1}*-Flag transgenes are well matched for expression levels, with *UAS-mid^{eh1}*-Flag expressed approximately twofold higher than *UAS-mid⁺*-Flag (Formaz-Preston et al., 2012; Svendsen et al., 2019). Thus, despite being expressed at a higher level than the *UAS-mid⁺*-Flag strain, the *UAS-mid^{eh1}*-Flag expressing clones have much weaker effects on pMad levels. Together, these results suggest that the eh1 domain is implicated in both of Mid's repressive roles: direct repression of Dpp-target genes and interference with the Dpp-signaling cascade.

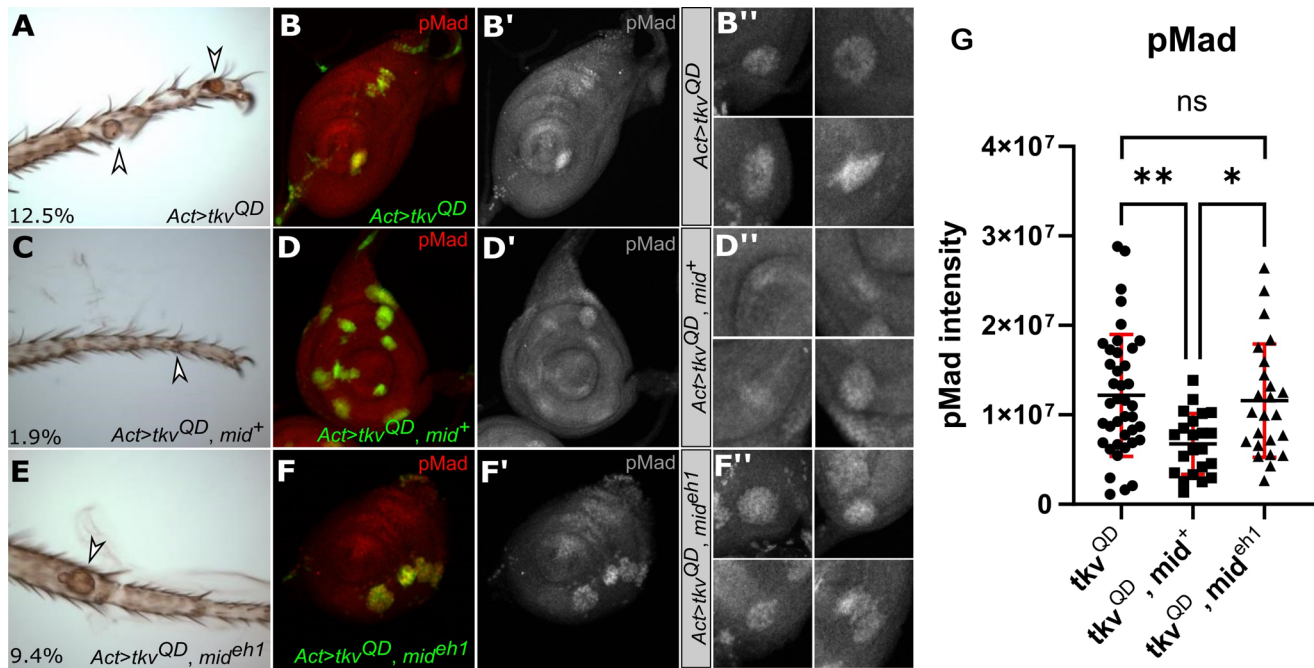


Fig. 4. The eh1 domain is involved in Dpp repression. (A) *AyGal4* gain-of-function clones expressing *UAS-tkv^{QD}* result in outgrowths and dorsal transformation (arrowhead), 12.5% of legs had ectopic outgrowths under these conditions ($n=181$). (C) When *UAS-tkv^{QD}* was co-expressed with *UAS-mid⁺-Flag*, the outgrowths were less severe (arrowhead) indicating suppression of the *tkv* gain-of-function phenotype. The effect was also less frequent with only 1.9% of legs having ectopic outgrowths ($n=309$). (E) Clones co-expressing *UAS-tkv^{QD}* and *UAS-mid^{eh1}-Flag* had deformities (arrowhead) similar to clones expressing *UAS-tkv^{QD}* alone, where 9.4% of legs had ectopic outgrowths ($n=106$). The clones scored in adult cuticles in panels A, C and E are not marked in these experiments but resemble the effect of marked *tkv^{QD}* clones in other experiments (data not shown). pMad staining (red, greyscale single channel) was upregulated in clones (green) expressing *UAS-tkv^{QD}* (B,B',B''; $n=40$) and clones co-expressing *UAS-tkv^{QD}* and *UAS-mid^{eh1}-Flag* (green) (F,F',F''; $n=24$). When *UAS-mid⁺-Flag* was expressed in clones (green) along with *UAS-tkv^{QD}*, pMad staining was less elevated (D,D',D''; $n=22$). (G) The difference in pMad levels staining between *UAS-tkv^{QD}* clones and *UAS-tkv^{QD}, UAS-mid^{eh1}-Flag* was not significant. However, clones expressing *UAS-tkv^{QD}*, *UAS-mid⁺-Flag* had significantly lower pMad compared to the other two conditions. The mean values were *UAS-tkv^{QD}* 1.22×10^7 , *UAS-tkv^{QD}, UAS-mid⁺-Flag* 6.73×10^6 and *UAS-tkv^{QD}, UAS-mid^{eh1}-Flag* 1.16×10^7 . Statistical analysis used the Tukey's multiple comparisons test, with bars representing the mean, s.d., and significance indicated, * P -value ≤ 0.05 and ** P -value ≤ 0.01 .

DISCUSSION

In this study, we investigated how the ventral selector gene *mid* antagonizes Dpp signaling. Specifically, we showed that *mid*, which antagonizes Dpp signaling and pMad accumulation, represses the Dpp-activated gene *Dad* but has minimal effects on the regulation of the Dpp-repressed gene *brk*. Furthermore, *mid* antagonizes dorsal fate by repressing *Dad* and by inhibiting Dpp signaling induced pMad accumulation via the eh1 domain.

We showed previously that Mid localizes to several *Dad* enhancers, including the *Dad13* enhancer, and represses a *Dad* enhancer trap in an eh1-dependent manner (Svendsen et al., 2019; unpublished data). Here we show that *mid* regulates *Dad13*-driven expression through a TBE site. Ventral *Dad13*-driven expression is increased and expanded in *mid* loss-of-function, while ectopic expression of *mid* blocks *Dad13*-reporter expression. Mutating the TBE in the *Dad13* enhancer fragment increased *Dad13* expression levels and expanded the ventral domain of expression compared with controls. Furthermore, the TBE mutation rendered the construct less sensitive to *mid⁺* gain-of-function. The localization of Mid to the *Dad13* enhancer by ChIP (Svendsen et al., 2019) and the genetic results suggesting that the TBE is required for Mid repression of *Dad13*-expression supports direct repression of *Dad* by Mid through the TBE.

However, a surprising result in light of this proposal was that the dorsal *Dad13^{TBE}*-driven expression outside the *mid* expression domain was also increased compared to *Dad13*. This suggests that the TBE sequence binds factors in dorsal cells to control the activity

of the *Dad13* enhancer. Recent work on *Tc-omb*, the *optomotor-blind* (*omb*) homolog in the red flour beetle, *Tribolium castaneum*, suggests one possible explanation. Like the *Drosophila* T-box factor *omb*, *Tc-omb* is expressed in the dorsal region of developing beetle legs and is required for dorsal patterning. Loss of function of dorsal *Tc-omb* results in increased pSmad levels in dorsal cells (Pechmann and Prpic, 2022). This is analogous to the increase in ventral pMad levels we find in *mid H15* loss of function (Svendsen et al., 2019). Although it is not known if *Tc-omb* loss of function also results in the increase of Dpp target genes in *T. castaneum*, it is interesting to speculate that perhaps dorsal T-boxes like *omb* play parallel roles to *mid* and *H15*, dorsal Dpp signaling and gene expression.

A second finding is that Mid suppresses pMad accumulation in a manner that is dependent on the eh1 domain. Mid mutants in which eh1 is compromised are unable to suppress Dpp gain-of-function effects. When co-expressed with Dpp-signaling overexpression in imaginal discs, clones of *UAS-mid^{eh1}-Flag* maintain strong pMad staining and adult cuticles display outgrowths and deformities that resemble the effects of Dpp-signaling overexpression alone. Conversely, clones activated for Dpp signaling that express wild-type *mid* (*UAS-mid⁺-Flag*) have decreased pMad levels in imaginal discs, while adult legs have fewer and milder defects. This demonstrates that in addition to blocking Dpp-target genes such as *Dad*, *mid* represses genes that act to increase pMad levels and Dpp signaling. What these repressed target genes may be remains a subject for further study.

Our results showing that *brk* expression was not affected by *mid* were surprising to us because *brk* is a sensitive readout of Dpp signaling and because *mid* alters pMad levels. However, *mid* loss-of-function clones, which increase pMad levels, do not affect *brk* expression, even though *brk* is regulated by Dpp-signaling in ventral *mid*-expressing cells. It seems likely that *brk* is simply not sensitive to the modulations in pMad seen in *mid/H15* mutant clones. Additionally, *mid* expression was unable to substantially reverse the repression of *brk* by Dpp gain-of-function, despite *mid* dramatically decreasing pMad accumulation in this genetic background, suggesting that *brk* repression is sensitive to repression at low thresholds of Dpp signaling. This suggests that, overall, *mid* and *H15* do not contribute to the regulation of *brk*.

The lack of interaction between *mid* and *brk* in this study is consistent with previous work, where it was reported that the expression of the ventral genes *H15* and *wg*, and the dorsal genes *omb* and *dpp*, were normal in *brk* mutant leg discs, indicating that *brk* does not participate in the formation of the DV axis (Estella and Mann, 2008). Instead, *brk* functions to form the proximo-distal (PD) axis by antagonizing the Wg target genes *Distalless* (*Dll*) and *dachshund* (*dac*), helping to establish their expression in the PD axis. This leads to a model in which Dpp induces the PD and DV leg axes through two separate modes: Dpp inhibits *brk* repression of Wg targets to establish the PD axis and antagonizes Wg targets in ventral development through pMad/Med/Shn mediated repression (Estella and Mann, 2008). Thus, *mid* and *brk* may play parallel roles repressing Dpp-target genes in the D/V and P/D axes of the leg imaginal disc, respectively.

MATERIALS AND METHODS

Fly stocks and constructs

All flies were maintained on standard media containing cornmeal, agar, yeast, glucose, and water (Deliu et al., 2017) and housed at between 18°C–25°C. Stocks UAS-*tkv^{9D}*, *brk-lacZ*, and *Dad-lacZ* were obtained from Bloomington Indiana Stock Center. *brk-lacZ* (BM315) was a gift from Dr. Konrad Basler, University of Zurich (Müller et al., 2003). *H15^{X4} mid^{1a5}*, UAS-*mid^{V5}*, (Svendsen et al., 2009) and UAS-*mid2.12* (Buescher et al., 2004) were generated previously.

UAS-*mid* strains

In this study, *mid⁺* may refer to either UAS-*mid^{V5}* or UAS-*mid2.12* and both lines have very similar levels of *mid⁺* activity. For quantitative comparisons of *mid⁺* and mutant *mid^{eh1}*, previously generated strains with Flag-tagged constructs, UAS-*mid^{eh1}*-Flag and UAS-*mid⁺*-Flag, were used (Formaz-Preston et al., 2012). The relative expression levels of these lines are such that *mid^{eh1}* is expressed at roughly two-fold higher levels than *mid⁺* (Formaz-Preston et al., 2012; Svendsen et al., 2019). UAS-*mid⁺* strains have generally stronger effects than UAS-*mid⁺*-Flag in gain-of-function experiments, although both UAS-*mid⁺* and UAS-*mid⁺*-Flag are able to rescue *mid H15* loss-of-function (Formaz-Preston et al., 2012; Svendsen et al., 2019).

Dad13 reporter strains

Dad13 constructs (Dad13, Dad13^{TBE}, Dad13^{SBE}, and Dad13^{SBE+TBE}) were generated for this study using the pGL3basic-hsp70-dad13 (331) plasmid gifted by Dr. Giorgos Pyrowolakis, University of Freiburg, and mutations were made with an adapted splice protocol (Warrens et al., 1997) in a placZ-2.attB vector. All transgenes were inserted into P{CaryP}attP2 located at 68A4. The Dad13nRFP strain was a gift from Dr. Doug Allan, University of British Columbia.

Loss-of-function and gain-of-function genetic mosaics

Heat shocking larvae 48–72 h after egg laying activates heat-shock-inducible hs-FLP, which is implemented in both gain-of-function and

loss-of-function clonal experiments. In gain-of-function experiments, the combination of an *AyGal4* construct with a UAS-linked gene allows for generation of ectopic clones which are labeled with GFP (Ito et al., 1997). Inducing the hs-FLP in loss-of-function experiments catalyzes mitotic recombination between FRT sites of homologous chromosomes (Xu and Rubin, 1993). This gives rise to two daughter cells homozygous for different genotypes, mutant and wild type. The consequent clones have wild-type cells marked with GFP, whereas loss-of-function cells lack GFP.

Reporter constructs, immunohistochemistry and imaging

The expression of *Dad-lacZ* (Tsuneizumi et al., 1997), *brk-lacZ* (Müller et al., 2003), and *Dad13* constructs were detected using mouse-anti-β-galactosidase (1:1000, Promega catalogue number Z3781) and rabbit-anti-β-galactosidase (1:1000, Cell Signaling Technology, catalogue number 27198). *Brk* was also detected with rat anti-Brk (1:100, a gift from Gines Morata, Universidad Autonoma de Madrid; Moreno et al., 2002). *Dad13* was visualized by RFP expression. pMad was detected with the rabbit-anti-pSmad1/5/9 antibody (1:200, Cell Signaling Technology, catalogue numbers S463/465/ S465/467, D5B10 13820S). Secondary antibodies used were Alexa-fluor 546 and 488 against rabbit, rat, or mouse (1:500, molecular probes A11029, lot 504513, A11094, lot 47207A, A11030, lot 517979, A11035, lot 584959, A11081, lot 58080A). Imaginal discs were imaged on a Zeiss LSM 700 confocal microscope using the 20x objective lens with ZEN 2.3 SP1 FP3 Black edition software. All compared genotypes were imaged at the same acquisition settings to maintain intensities. Adult tissues were visualized on a Leica MPS60 compound microscope with a 10x or 20x objective and QCapture_x64 software. Z-stack CZI files generated on the Zeiss LSM 700 Axio Observer confocal microscope were processed and analyzed with ImageJ software (version 1.53c, Java 1.8.0_172, 64-bit) and saved as JPEG files. Some files were then further analyzed to determine fluorescence intensity in according to published methods (McCloy et al., 2014). Images were imported into INKScape (version 1.0.2-2, e86c870879, 2021-01-15) to generate figures for this paper. Graphs were generated and statistical analysis performed in GraphPad Prism (version 9.2.0) using either unpaired *t*-test (Figure 2) or ordinary one-way analysis of variance (ANOVA) (Figure 4) with Tukey's multiple comparisons test.

Acknowledgements

We thank Doug Allan (University of British Columbia), Konrad Basler (University of Zurich) and the Indiana Stock Center for the *Drosophila* strains used in this study. We thank Gines Morata, (Universidad Autonoma de Madrid) for the *brk* antibody and Giorgos Pyrowolakis (University of Freiburg) for the plasmid containing *Dad13*. We thank BestGene Inc. (Chino Hills, CA, USA) for the transgene injection services.

Competing interests

The authors declare no competing or financial interests.

Author contributions

Conceptualization: L.A.P., W.J.B.; Methodology: L.A.P., J.-R.R., P.C.S., W.J.B.; Validation: L.A.P.; Formal analysis: L.A.P., M.L.A.; Investigation: L.A.P., M.L.A., L.K.K., P.C.S.; Writing - original draft: L.A.P., M.L.A.; Writing - review & editing: L.A.P., P.C.S., W.J.B.; Visualization: L.A.P.; Supervision: L.A.P., W.J.B.; Project administration: L.A.P., W.J.B.; Funding acquisition: W.J.B.

Funding

This work was supported by a National Sciences and Engineering Research Council of Canada (RGPIN/04828-2017 to W.J.B.). LAP was funded by an Alberta Children's Hospital Research Institute Award. L.K.K. and M.L.A. were supported by National Sciences and Engineering Research Council of Canada summer awards. Open Access funding was provided by University of Calgary. Deposited in PMC for immediate release. Open access funding was provided by NSERC.

References

- Buescher, M., Svendsen, P. C., Tio, M., Miskolczi-McCallum, C., Tear, G., Brook, W. J. and Chia, W. (2004). *Drosophila* T box proteins break the symmetry of hedgehog-dependent activation of wingless. *Curr. Biol.* **14**, 1694–1702. doi:10.1016/j.cub.2004.09.048
- Deliu, L. P., Ghosh, A. and Grewal, S. S. (2017). Investigation of protein synthesis in *Drosophila* larvae using puromycin labelling. *Biol. Open* **6**, 1229–1234. doi:10.1242/bio.026294

- Estella, C. and Mann, R. S.** (2008). Logic of Wg and Dpp induction of distal and medial fates in the *Drosophila* leg. *Development* **135**, 627-636. doi:10.1242/dev.014670
- Formaz-Preston, A., Ryu, J.-R., Svendsen, P. C. and Brook, W. J.** (2012). The Tbx20 homolog Midline represses wingless in conjunction with Groucho during the maintenance of segment polarity. *Dev. Biol.* **369**, 319-329. doi:10.1016/j.ydbio.2012.07.004
- Gao, S., Steffen, J. and Laughon, A.** (2005). Dpp-responsive silencers are bound by a trimeric Mad-Medea complex. *J. Biol. Chem.* **280**, 36158-36164. doi:10.1074/jbc.M506882200
- Hamaratoglu, F., Affolter, M. and Pyrowolakis, G.** (2014). Dpp/BMP signaling in flies: from molecules to biology. *Semin. Cell Dev. Biol.* **32**, 128-136. doi:10.1016/j.semcdb.2014.04.036
- Held, L. I. and Heup, M. A.** (1996). Genetic mosaic analysis of decapentaplegic and wingless gene function in the *Drosophila* leg. *Dev. Genes Evol.* **206**, 180-194. doi:10.1007/s004270050044
- Hudson, J. B., Podos, S. D., Keith, K., Simpson, S. L. and Ferguson, E. L.** (1998). The *Drosophila* Medea gene is required downstream of dpp and encodes a functional homolog of human Smad4. *Development* **125**, 1407-1420. doi:10.1242/dev.125.8.1407
- Ito, K., Awano, W., Suzuki, K., Hiromi, Y. and Yamamoto, D.** (1997). The *Drosophila* mushroom body is a quadruple structure of clonal units each of which contains a virtually identical set of neurones and glial cells. *Development* **124**, 761-771. doi:10.1242/dev.124.4.761
- Kim, J., Johnson, K., Chen, H. J., Carroll, S. and Laughon, A.** (1997). *Drosophila* mad binds to DNA and directly mediates activation of vestigial by decapentaplegic. *Nature* **388**, 304-308. doi:10.1038/40906
- Manjón, C., Sánchez-Herrero, E. and Suzanne, M.** (2007). Sharp boundaries of Dpp signalling trigger local cell death required for *Drosophila* leg morphogenesis. *Nat. Cell Biol.* **9**, 57-63. doi:10.1038/ncb1518
- Mann, R. S. and Morata, G.** (2000). The developmental and molecular biology of genes that subdivide the body of *Drosophila*. *Annu. Rev. Cell Dev. Biol.* **16**, 243-271. doi:10.1146/annurev.cellbio.16.1.243
- Marty, T., Müller, B., Basler, K. and Affolter, M.** (2000). Schnurri mediates Dpp-dependent repression of brinker transcription. *Nat. Cell Biol.* **2**, 745-749. doi:10.1038/35036383
- McCloy, R. A., Rogers, S., Caldon, C. E., Lorca, T., Castro, A. and Burgess, A.** (2014). Partial inhibition of Cdk1 in G2 phase overrides the SAC and decouples mitotic events. *Cell Cycle* **13**, 1400-1412. doi:10.4161/cc.28401
- Moreno, E., Basler, K. and Morata, G.** (2002). Cells compete for decapentaplegic survival factor to prevent apoptosis in *Drosophila* wing development. *Nature* **416**, 755-759. doi:10.1038/416755a
- Müller, B., Hartmann, B., Pyrowolakis, G., Affolter, M. and Basler, K.** (2003). Conversion of an extracellular Dpp/BMP morphogen gradient into an inverse transcriptional gradient. *Cell* **113**, 221-233. doi:10.1016/S0092-8674(03)00241-1
- Najand, N., Ryu, J.-R. and Brook, W. J.** (2012). In vitro site selection of a consensus binding site for the *Drosophila melanogaster* Tbx20 Homolog midline. *PLoS ONE* **7**, e48176. doi:10.1371/journal.pone.0048176
- Pechmann, M. and Prpic, N.-M.** (2022). The T-box gene optomotor-blind organizes proximodistal leg patterning in the beetle *Tribolium castaneum* by repressing dorsal Dpp pathway activity. *Dev. Biol.* **482**, 124-134. doi:10.1016/j.ydbio.2021.12.008
- Saller, E. and Bienz, M.** (2001). Direct competition between Brinker and *Drosophila* Mad in Dpp target gene transcription. *EMBO Rep.* **2**, 298-305. doi:10.1093/embo-reports/kve068
- Svendsen, P. C., Formaz-Preston, A., Leal, S. M. and Brook, W. J.** (2009). The Tbx20 homologs midline and H15 specify ventral fate in the *Drosophila melanogaster* leg. *Development* **136**, 2689-2693. doi:10.1242/dev.037911
- Svendsen, P. C., Ryu, J. R. and Brook, W. J.** (2015). The expression of the T-box selector gene midline in the leg imaginal disc is controlled by both transcriptional regulation and cell lineage. *Biol. Open* **4**, 1707-1714. doi:10.1242/bio.013565
- Svendsen, P. C., Phillips, L. A., Deshwar, A. R., Ryu, J. R., Najand, N. and Brook, W. J.** (2019). The selector genes midline and H15 control ventral leg pattern by both inhibiting Dpp signaling and specifying ventral fate. *Dev. Biol.* **455**, 19-31. doi:10.1016/j.ydbio.2019.05.012
- Tsuneizumi, K., Nakayama, T., Kamoshida, Y., Kornberg, T. B., Christian, J. L. and Tabata, T.** (1997). Daughters against dpp modulates dpp organizing activity in *Drosophila* wing development. *Nature* **389**, 627-631. doi:10.1038/39362
- Warrens, A. N., Jones, M. D. and Lechler, R. I.** (1997). Splicing by over-lap extension by PCR using asymmetric amplification: an improved technique for the generation of hybrid proteins of immunological interest. *Gene* **186**, 29-35. doi:10.1016/S0378-1119(96)00674-9
- Weiss, A., Charbonnier, E., Ellertsdóttir, E., Tsirigos, A., Wolf, C., Schuh, R., Pyrowolakis, G. and Affolter, M.** (2010). A conserved activation element in BMP signaling during *Drosophila* development. *Nat. Struct. Mol. Biol.* **17**, 69-77. doi:10.1038/nsmb.1715
- Xu, T. and Rubin, G. M.** (1993). Analysis of genetic mosaics in developing and adult *Drosophila* tissues. *Development* **117**, 1223-1237. doi:10.1242/dev.117.4.1223